

Collisional properties of ultracold K-Rb mixtures

G. Ferrari, M. Inguscio*, W. Jastrzebski†, G. Modugno, G. Roati‡

INFN and European Laboratory for Nonlinear Spectroscopy, Università di Firenze, 50019 Firenze, Italy

A. Simoni

INFN and Dipartimento di Chimica, Università di Perugia, 06123 Perugia, Italy

(May 21, 2019)

We determine the inter-species *s*-wave triplet scattering length a_3 for all K-Rb isotopic mixtures by measuring the cross-section for collisions between ^{41}K and ^{87}Rb in different temperature regimes. The positive value $a_3 = +163^{+57}_{-12} a_0$ ensures the stability of binary ^{41}K - ^{87}Rb Bose-Einstein condensates. For the fermion-boson mixture ^{40}K - ^{87}Rb we obtain a large and negative scattering length which implies an efficient sympathetic cooling of the fermionic species down to the degenerate regime.

34.50.-s, 34.50.Pi, 05.30.Jp, 05.30.Fk, 32.80.Pj

Ultracold mixtures of alkali atoms have recently been the subject of intensive experimental research, mainly aimed at the production of novel degenerate quantum systems. Sympathetic cooling [1] in a mixture represents a way to reach the degenerate regime for species which cannot be efficiently cooled by direct evaporation, as in the case of ^6Li [2] and ^{41}K [3]. In addition, mixing different isotopes or atomic species allows to create ultracold Bose-Fermi systems [4,5], and paves the way to the creation of binary Bose-Einstein condensates with different atomic species and of ultracold heteronuclear molecules.

In an ultracold mixture the interaction between the components is described in terms of a single key parameter, the inter-species *s*-wave scattering length, which for example determines the efficiency of the sympathetic-cooling procedure. In addition, knowledge of the scattering length is important in order to predict macroscopic properties of these mixed systems, such as the stability and phase separation of binary degenerate systems, or microscopic properties, such as the occurrence of Feshbach resonances in the inter-species collisions. While collisions either between alkali of the same species or between different isotopes have often been well characterized [6], collisions between different alkali species represent a still relatively unexplored field.

In this context, K-Rb mixtures are particularly inter-

esting, since they are promising candidates in the general field of Bose-Fermi and Bose-Bose degenerate gases. Despite this interest, an accurate characterization of K-Rb collisions is lacking and only the magnitude of the ^{41}K - ^{87}Rb *s*-wave triplet scattering length has been estimated [3]. In this Letter we report the results of a thorough investigation of the collisional properties of a ^{41}K - ^{87}Rb mixture. By studying the interspecies elastic collisions in a broad temperature range, we determine the sign of the scattering length and tighten the bounds on its magnitude. Thanks to this result, we are able to derive by mass scaling the triplet scattering lengths for all the other combinations of K and Rb stable isotopes and to discuss the possibility of producing mixed K-Rb degenerate systems. We also determine a region of confidence for the singlet *s*-wave scattering length of the ^{41}K - ^{87}Rb mixture from inelastic decay rates of a mixed-spin sample.

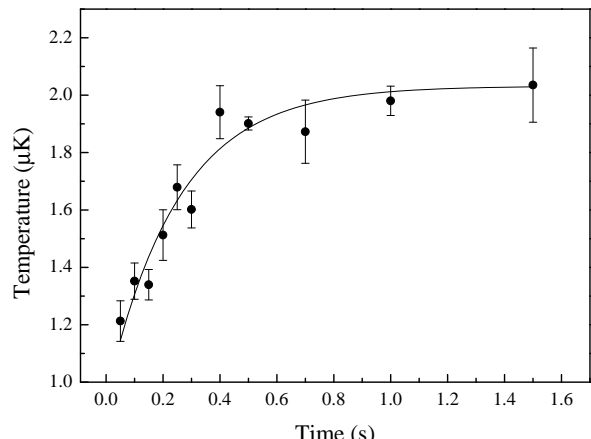


FIG. 1. Evolution of the mean temperatures of the K sample after 100 ms of selective heating of Rb. Each datapoint is the average of five measurements, and the error bar displays the corresponding statistical fluctuation. The continuous line is the best fit to an exponential function; the time-constant is inversely proportional to the K-Rb elastic collisional rate.

The ultracold ^{41}K - ^{87}Rb mixture is produced using the apparatus described in [3]. In brief, about 10^7 K atoms at $300 \mu\text{K}$ and 5×10^8 Rb atoms at $100 \mu\text{K}$ are loaded in a QUIC magnetostatic trap [7] using a double-magneto-optical trap scheme. Both species are prepared in their doubly-polarized spin state $|F = 2, M_F = 2\rangle$ thanks to an

*also at Dipartimento di Fisica, Università di Firenze, 50019 Firenze, Italy.

†also at Institute of Physics, Polish Academy of Science, 02668 Warszawa, Poland

‡also at Dipartimento di Fisica, Università di Trento, 38050 Povo, Italy

optical pumping stage. A gas prepared in such state has the advantage of being immune to spin-exchange losses and is typically stable. Evaporative cooling is then performed selectively on the Rb sample using a microwave knife tuned to the hyperfine transition at 6.8 GHz (the corresponding transition for K is at 254 MHz), while the K sample is sympathetically cooled through elastic K-Rb collisions. The number of atoms and temperature of both samples is determined simultaneously at the end of each experimental run by absorption imaging, using two delayed resonant light pulses after release from the magnetic trap. Both atomic species experience the same trapping potential with cylindrical symmetry. The axial and radial harmonic frequencies for Rb are $\omega_{ax} = 2\pi \times 16.3 \text{ s}^{-1}$ and $\omega_{rad} = 2\pi \times 197 \text{ s}^{-1}$ respectively, while those for K are by a factor $(M_{Rb}/M_K)^{1/2} = 1.45$ larger.

We have investigated the dependence of the K-Rb elastic cross-section on temperature, by performing a series of rethermalization measurements. We drive the system out of thermal equilibrium and observe the subsequent thermalization mediated by elastic collisions. The different trap frequencies for the two species allow us to selectively heat Rb by superimposing a 10% modulation on the trapping potential at twice the Rb radial frequency for typically 100 ms. As an example we show in Fig. 1 the measured increase of temperature of the K sample at $T \approx 1.6 \mu\text{K}$ that follows heating of Rb, together with an exponential fit to the data. The time constant for rethermalization τ is determined from the fit. We have checked that the aspect ratio of the K sample was constant during the whole rethermalization which is evidence for a common temperature of the spatial degrees of freedom.

We plot in Fig. 2 the measured elastic-collision rate $1/(\tau\bar{n})$ as a function of temperature in the range $(1.6 - 45) \mu\text{K}$. Here $\bar{n} = (\frac{1}{N_K} + \frac{1}{N_{Rb}}) \int n_K n_{Rb} d^3x$ is the effective density of K and Rb atoms.

A general model to describe the thermalization between atoms of different masses can be obtained by extending the one of Ref. [8] to energy-dependent cross sections and to partial waves higher than s -wave. We have checked that at our temperatures only s - and p -wave collisions are relevant. The thermalization time per unit atomic density mediated by s - and p - wave collisions is

$$\frac{1}{\tau\bar{n}} = \frac{\xi}{2\alpha_s k_B T} \left[\langle \sigma_s v E \rangle + \frac{\alpha_s}{\alpha_p} \langle \sigma_p v E \rangle \right], \quad (1)$$

where $\alpha_s \simeq 2.7$ is the average number of s -wave collisions necessary for rethermalization, v is the relative velocity of a colliding pair and E is the relative collision energy. We obtain the ratio $\frac{\alpha_s}{\alpha_p} = \frac{3}{5}$ upon integration over all collision directions. The factor $\xi = 4\mu/M$, with M and μ the total and the reduced mass respectively, gives a reduction $\xi \simeq 0.87$ of the thermalization efficiency with respect to the case of equal masses. Finally, the averages $\langle \cdot \rangle$ are performed on a classical Maxwell-Boltzmann distribution of relative velocities.

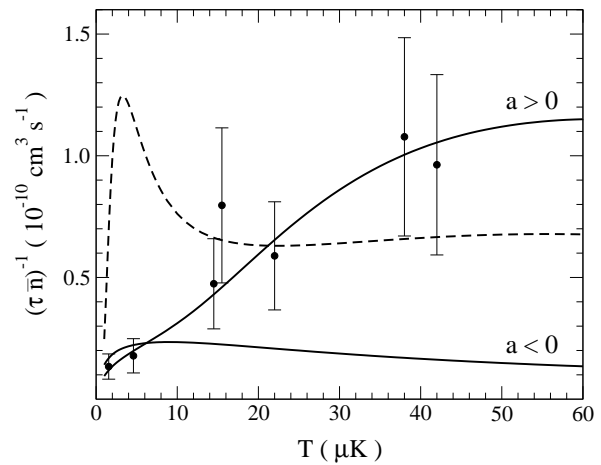


FIG. 2. Dependence on temperature of the elastic collision rate $1/(\tau\bar{n})$. The points are the experimental data. The solid lines are the best fit to the model described in the text for positive and negative triplet scattering lengths, corresponding to $a_3 = 163 a_0$ and $a_3 = -209 a_0$, respectively. The dashed line corresponds to $a_3 = 140 a_0$.

The partial cross sections are obtained from a numerical solution of the scattering equations using standard propagation algorithms. The molecular Hamiltonian for collisions of atoms with hyperfine structure includes the kinetic energy of the relative motion, the hyperfine atomic energy and the adiabatic Born-Oppenheimer $^1\Sigma_g^+$ and $^3\Sigma_u^+$ symmetry potentials. The latter have been constructed by smoothly matching the short-range *ab initio* potential of [9] onto a long-range analytic potential $V = V_d \pm V_{ex}/2$. Here $V_d = -C_6/R^6 - C_8/R^8 - C_{10}/R^{10}$ is the dispersion potential and V_{ex} is the exchange potential. An accurate van-der-Waals coefficient C_6 is taken from Ref. [10], C_8 and C_{10} from [11] and the analytic form of V_{ex} from [12]. The molecular potential is made flexible by adding a short-range correction to the adiabatic potentials (see Ref. [13]). This procedure allows us to tune singlet and triplet scattering lengths to agree with the data.

The experimental data are fitted using a min- χ^2 procedure. Since collisions between atoms prepared in a doubly-polarized spin state are single-channel collisions involving only the $^3\Sigma_u^+$ symmetry potential, the scattering length a_3 is the only free parameter in the model [14]. Our main results are shown in Fig. 2. The best agreement is obtained for a positive scattering length $a_3 = 163 a_0$, while the best-fit curve for negative a_3 fails to fit the experiment at high temperature (solid lines in Fig. 2). Actually, for $a_3 < 0$ the cross-section drops with energy from its threshold value $\sigma_s = 4\pi a_3^2$ at lower collision energies than it does for $a_3 > 0$. Moreover, the curve for $a_3 = 163 a_0$ has a significant contribution from a broad p -wave shape-resonance near the top of the centrifugal barrier which further increases the rate at high T . This resonance rapidly shifts at lower energies for decreasing a_3 (dashed line in Fig. 2). This circumstance and the

absence of observed resonant features sets a tight lower bound $a_3 \approx 150 a_0$ on the confidence interval for a_3 , while the upper bound is looser. Actually, scattering lengths $a_3 \approx 200 a_0$ having only a minor p -wave contribution still agree well with the data.

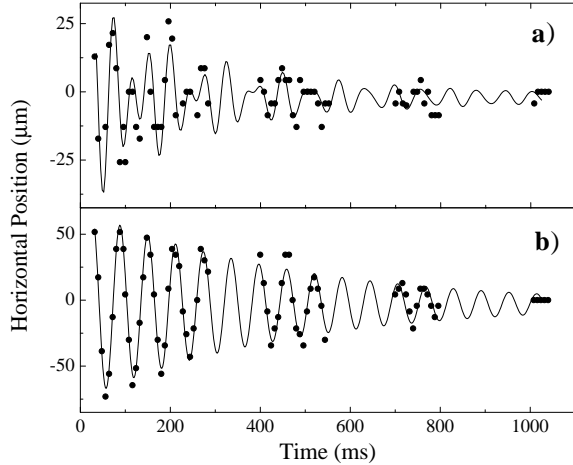


FIG. 3. Dipole oscillations of the K (a) and Rb (b) clouds along the weak trap axis. The solid lines are a best fit to the model presented in the text. The faster damping and the beatings observed in the K motion are due to the smaller mass of the K sample.

In order to confirm our determination of the magnitude of a_3 we have performed an independent measurement of the collisional cross-section, studying the damping of dipole oscillations of a sample composed by 8×10^4 K atoms and 1.5×10^5 Rb atoms, at $T = 1.7 \mu\text{K}$. Dipolar modes of the two atomic clouds are excited by displacing the potential minimum along the weak horizontal trap axis for about 30 ms. As shown in Fig. 3 the center of mass oscillations get rapidly coupled and damped by elastic collisions. We fit the experimental data to the solutions of the coupled equations of motion for the clouds centers of mass

$$\begin{aligned} \ddot{z}_1 &= -\omega_1^2 z_1 - \frac{4}{3} \frac{M_2}{M} \frac{N_2}{N} \Gamma (\dot{z}_1 - \dot{z}_2) \\ \ddot{z}_2 &= -\omega_2^2 z_2 + \frac{4}{3} \frac{M_1}{M} \frac{N_1}{N} \Gamma (\dot{z}_1 - \dot{z}_2), \end{aligned} \quad (2)$$

where the labels 1 and 2 denote K and Rb respectively, $M = M_1 + M_2$, $N = N_1 + N_2$, $\Gamma = \bar{n} \sigma_s v$ is the s -wave collision rate, v is the rms relative velocity, and \bar{n} is the atoms density defined above. The low temperature at which the experiment is performed ensures that s -wave collisions dominate. Our system appears to be in the collisionless regime ($\Gamma \ll \omega_1, \omega_2$), where the position of each center of mass is the sum of two damped sinusoids at the bare frequencies of K and Rb. Our best fit, shown in Fig. 3, well reproduces the experimental observation. From the fitted collision rate $\Gamma = 5.2(7) \text{ s}^{-1}$ we determine the magnitude of triplet scattering length

$|a_3| = 170^{+35}_{-35} a_0$, where the uncertainty is dominated by that on the atom number. This value for $|a_3|$ is in good agreement with the one previously derived from thermalization measurements.

We determine the singlet K-Rb scattering length a_1 , by measuring the trap loss for collision between K atoms in the hyperfine state $|2, 2\rangle$ and Rb atoms in $|2, 1\rangle$. Our sample is initially composed by a small number of K atoms (3×10^4) and a larger number of Rb atoms (1.2×10^5), both in $|2, 2\rangle$, at a temperature $T = 1.8 \mu\text{K}$. We then transfer a small fraction (20%) of both species in $|2, 1\rangle$ using a radio-frequency sweep and we study the subsequent decay of K, which takes place on a timescale much shorter than the lifetime of the doubly spin-polarized mixture. In these experimental conditions K atoms in $|2, 1\rangle$ and Rb atoms in $|2, 2\rangle$ do not contribute significantly to loss of K atoms from the trap. The time evolution of K-atoms number is given to a good approximation by the solution of the single rate equation $\dot{n}^K(t) = -G n_{|2,2\rangle}^K(t) n_{|2,1\rangle}^{Rb}(t)$ with the constraint $N_{|2,2\rangle}^K(t) - N_{|2,1\rangle}^{Rb}(t) = \text{const}$. Here n is the spatial density, N the atom number and G is the rate constant for inelastic collisions between K in $|2, 2\rangle$ and Rb in $|2, 1\rangle$ [15]. Our collision model agrees well with the experimental data for an inelastic collision rate $G = 1.8(9) \times 10^{-11} \text{ cm}^3 \text{ s}^{-1}$. A comparison between the measured inelastic rate and the numerical calculation (shown in Fig. 4) allows us to determine the region of confidence for the singlet scattering length a_1 , given our interval of a_3 values. This comparison singles out a region of positive singlet scattering length, $a_1 > 30 a_0$, excluding a broad region of strong suppression of inelastic processes centered at $a_1 \sim a_3$. In alternative, the large negative singlet scattering length $a_1 < -210 a_0$ is also compatible with the data.

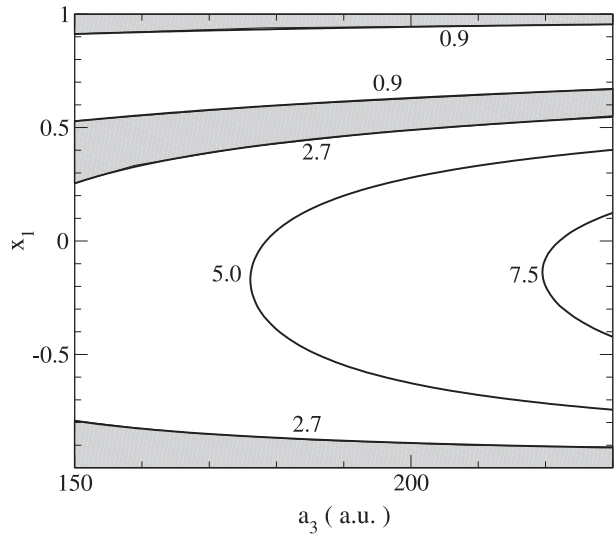


FIG. 4. Contour plot of the calculated inelastic collisional rate G in units of $10^{-11} \text{ cm}^3 \text{ s}^{-1}$ vs the triplet scattering length a_3 and the reduced singlet scattering length $x_1 = 2/\pi \arctan(a_1/a_{sc})$, where $a_{sc} = 72 a_0$. The shaded regions correspond to the rate determined in the experiment.

This result represents a first characterization of the singlet K-Rb interaction, and can provide a useful guidance for further collisional studies, in particular for the investigation of Feshbach resonances in selected spin-states.

We have also determined the triplet *s*-wave scattering lengths for all the other pairs of K and Rb isotopes. It must be remarked that while our results for ^{41}K - ^{87}Rb are to a large extent independent on the number N_b of bound states supported by the triplet potential, scaling from one isotope to the others does depend on N_b . Tab. I summarizes our results for the nominal number of bound states $N_b = 32$ in the triplet potential. Calculations that allow for a realistic (± 2) uncertainty in N_b do not qualitatively change the results of Tab. I. With this proviso, we discuss below the consequences of these results.

The repulsive character of the ^{41}K - ^{87}Rb triplet interaction indicates that it is possible to form a stable binary Bose-Einstein condensate. Indeed, in case of a *negative* inter-species scattering length much larger in magnitude than the single-species ones [16], the mean-field interaction would lead to a collapse of the condensates [19,20]. Of great interest is also the ^{40}K - ^{87}Rb pair, for which we find a negative and probably large inter-species scattering length. Therefore, at least in the absence of unfortunately placed zeros in the elastic cross section, sympathetic cooling of fermionic K with ^{87}Rb can be expected to be highly efficient. Moreover, the attractive character of the interaction should prevent phase separation of the two components once the degenerate regime has been reached [21], thus insuring an efficient thermalization even in this regime. This represents a qualitatively different situation with respect to the other known Bose-Fermi mixture, ^6Li - ^7Li , for which the interspecies scattering length is positive [22]. We note that among the pairs containing ^{85}Rb , which however does not seem to be an easy partner for sympathetic cooling [23], only the ^{41}K - ^{85}Rb pair shows a significantly large interaction. Finally, the mixture ^{39}K - ^{87}Rb is not particularly appealing, since the interspecies scattering length is expected to be relatively small and, moreover, the formation of a stable Bose-Einstein condensate of ^{39}K with a large number of atoms is prevented by the negative sign of its own scattering length [17].

In conclusion we have drawn a picture of the triplet interaction between all the K-Rb isotopes pairs. Our study paves the way to the production of novel mixtures of degenerate atomic gases, such as Bose-Bose systems with large repulsive interaction and Bose-Fermi systems with attractive interactions. Moreover, it provides important information for predicting the occurrence of magnetically-tunable Feshbach resonances. These resonances would represent a tool to control the inter-species interactions and to drive the production of ultracold heteronuclear molecules.

We are grateful to P. S. Julienne, F. H. Mies, E. Tiesinga, and C. J. Williams for the ground-state collisions code and several useful discussions. This work was supported by MURST, by ECC under the Contract

HPRICT1999-00111, and by INFM, PRA "Photonmatter".

TABLE I. Triplet *s*-wave scattering lengths (in a.u.) for collisions between K and Rb isotopes computed using the nominal triplet potential.

	^{39}K	^{40}K	^{41}K
^{85}Rb	58_{-6}^{+14}	-38_{-17}^{+37}	329_{-55}^{+1000}
^{87}Rb	31_{-6}^{+16}	-261_{-159}^{+170}	163_{-12}^{+57}

[1] D. J. Wineland, R. E. Drullinger, F. L. Walls, Phys. Rev. Lett. **40**, 1639 (1978).

[2] G. Truscott *et al.*, Science **291**, 2570 (2001).

[3] G. Modugno *et al.*, Science **294**, 1320 (2001).

[4] F. Schreck *et al.*, Phys. Rev. Lett. **87**, 080403 (2001).

[5] Z. Hadzibabic *et al.*, cond-mat/01112425.

[6] For a review see: J. Weiner, V. S. Bagnato, S. Zilio and P. Julienne, Rev. of Mod. Phys. **71**, 1 (1999).

[7] T. Esslinger, I. Bloch, T.W. Hänsch, Phys. Rev. A **58**, R2664 (1998).

[8] A. Mosk *et al.*, Appl. Phys. B **73**, 791 (2001), and references therein.

[9] A. Yannopoulou, T. Leininger, A. M. Lyyra, and G. H. Jeung, Int. J. Quant. Chem. **57**, 575 (1996).

[10] A. Dervianko, J. F. Babb, and A. Dalgarno, Phys. Rev. A **63**, 052704 (2001).

[11] M. Marinescu and H. R. Sadeghpour, Phys. Rev. A **59** 390 (1999).

[12] B. M. Smirnov and M. I. Chibisov, Sov. Phys. JETP **21**, 624 (1965).

[13] E. Tiesinga *et al.*, J. Res. Natl. Inst. Stand. Technol. **101**, 505 (1996).

[14] We have checked that a $\pm 1\%$ uncertainty in the highly accurate C_6 coefficient adopted in this work does not affect the results of the paper.

[15] The only relevant inelastic processes involved are $|2, 1\rangle + |2, 2\rangle \rightarrow |2, 2\rangle + |1, 1\rangle$ and $|2, 1\rangle + |2, 2\rangle \rightarrow |1, 1\rangle + |2, 2\rangle$.

[16] The triplet scattering lengths for ^{41}K and ^{87}Rb are $a_3 = 60 a_0$ [17] and $a_3 = 99 a_0$ [18], respectively.

[17] H. Wang *et al.*, Phys. Rev. A **62**, 052704 (2000).

[18] E.G.M. van Kempen, S.J.J.M.F. Kokkelmans, D.J. Heinzen, B.J. Verhaar, cond-mat/0110610.

[19] B. D. Esry *et al.*, Phys. Rev. Lett **78**, 3594 (1997); C. K. Law, *et al.*, Phys. Rev. Lett **79**, 3105 (1997); E. Timmermans, Phys. Rev. Lett **81**, 5718 (1998).

[20] Actually, simultaneous condensation of K and Rb has been observed: G. Roati, F. Riboli, G. Modugno, and M. Inguscio, in preparation.

[21] K. Mølmer, Phys. Rev. Lett. **80**, 1804 (1998).

[22] F. A. van Abeelen, B. J. Verhaar, and A. J. Moerdijk, Phys. Rev. A **55**, 4377 (1997).

[23] J. P. Burke *et al.*, Phys. Rev. Lett. **80**, 2097 (1998); S. L. Cornish *et al.*, Phys. Rev. Lett. **85**, 1795 (2000).